JOURNAL OF CATALYSIS 115, 376–387 (1989)

Potassium's Promotional Effect of Unsupported Copper Catalysts for Methanol Synthesis

GORDON R. SHEFFER AND TERRY S. KING

Department of Chemical Engineering, Iowa State University, Ames, Iowa 50011

Received February 29, 1988; revised September 13, 1988

This paper presents an investigation of the promotional effect of potassium on unsupported copper catalysts for the hydrogenation of carbon monoxide. Using X-ray photoelectron spectroscopy (XPS), we determined that under reaction conditions copper exists as a mixture of Cu^+ and Cu^0 species. Metallic copper by itself is inactive for the hydrogenation of carbon monoxide, while we have found that the addition of potassium to copper forms an active and selective (up to 98 wt %) methanol synthesis catalyst. The initiation of catalytic activity correlated with the stabilization of the Cu^+ species. The potassium promoter was determined to be in the form of the thermodynamically stable carbonate. Potassium promotes this catalyst by stabilizing the Cu^+ species, probably in the form of $CuKCO_3$.

INTRODUCTION

Audibert and Raineau (*1*) suspected as early as 1928 that traces of Group IA elements may promote the formation of methanol over copper metal. This suspicion resulted from their observation that copper catalysts prepared by precipitation using alkali hydroxide resulted in the synthesis of methanol, while those precipitated by ammonium hydroxide were inactive. However, when the addition of alkali to ammonium hydroxide precipitated catalysts proved ineffective, the researchers concluded that there was no connection between activity and alkali content. Instead, they suggested that reduced cupric or cuprous oxide alone renders an active methanol catalyst.

Later Eguchi (*2*) suggested that the addition of trace amounts of alkali to cupric oxide did produce a very active and selective methanol synthesis catalyst. However, Eguchi found that pure copper oxide that had been reduced was unable to produce methanol under any conditions. The inertness of unsupported copper metal toward carbon monoxide hydrogenation has been recently supported by the work of Klier (*3*).

Vedage *et al.* (*4*) have reported that the incorporation of alkali hydroxides into copper–zinc oxide methanol catalysts improved the synthesis rate. Cesium was found to be the best Group IA promoter with a twofold increase in rate over the unpromoted catalyst being observed. It was suggested that the role of cesium was to increase the concentration of surface hydroxyl groups that react with carbon monoxide to produce intermediate formate species. The formate species were then reduced by hydrogen to form methanol and regenerate surface hydroxyls (*5–7*).

In our laboratory we have recently investigated the promotional effect of potassium on unsupported copper catalysts for the hydrogenation of carbon monoxide. We have found that potassium promoted copper catalysts are active and selective catalysts for the synthesis of methanol. In this paper we report the results of the detailed characterization of various potassium promoted catalysts by powder X-ray diffraction (XRD), X-ray photoelectron spectroscopy (XPS), and scanning electron microscopy (SEM) with energy-dispersive spectroscopy (EDS). Microreactor studies of the variation in catalytic behavior with potassium promotion are also reported. The purpose of this study was to determine the interac-

0021-9517/89 $3.00

tion between potassium and copper that was responsible for the formation of a methanol catalyst. Specifically, the chemical state of both copper and potassium and the manner by which promotion occurs have been examined.

METHODS

Catalysts were prepared by methods similar to those outlined by Courty *et al.* (*8*). Briefly, citric acid was added to aqueous solutions of cupric nitrate and potassium nitrate to yield one gram equivalent of acid per gram equivalent of copper and potassium. The resulting solution was evaporated under vacuum at room temperature to form a thick slurry. The slurry was dried overnight at 353 K. The solid obtained was then calcined at 623 K in air for 4 hr. It was observed that at approximately 473 K the catalyst precursor rapidly decomposed with the evolution of large amounts of heat and gas. The potassium-to-copper molar ratio of the calcined catalysts was verified by flame emission and atomic absorption spectroscopies.

For purposes of comparison, two alternate preparation procedures were used. The first used the same technique as outlined above except that cupric acetate was substituted for cupric nitrate. The second procedure was a direct impregnation of reagent grade cupric oxide with an aqueous solution of potassium carbonate.

All catalysts were tested in a single-pass, fixed-bed, flow microreactor system outlined in Fig. 1. The unit was designed for operation up to 623 K and 15 MPa. Feed gases were H_2 (>99.995%), Ar (>99.9995%), and CO (>99.3%), which were further purified with molecular sieve 4A. Gases were metered by use of Brooks mass flow controllers.

The reaction vessel consisted of a 0.25-m, type 304 stainless-steel tube of 0.0092 m i.d. The amount of reaction occurring on the reactor and tubing walls in the system was found to be negligible by blank runs where the reactor was filled with powdered quartz. An air-fluidized aluminum oxide bath regulated by a time-proportional controller was used to maintain reactor temperature. The internal reactor temperature was measured by a subminiature thermocouple moved within a stainless-steel protection sheath positioned axially in the reactor.

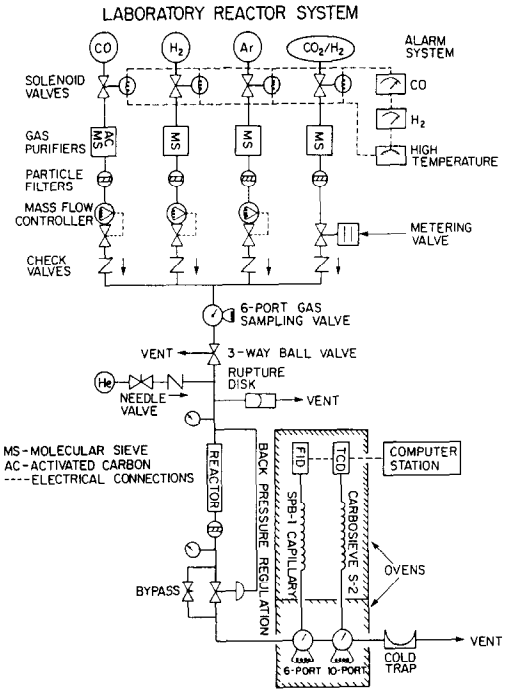

FIG. 1. Diagram of high-pressure microreactor system.

An air-actuated pressure control valve downstream from the reactor was used to maintain elevated reactor pressure. The controller for the valve sensed the inlet reactor pressure in order to avoid condensation of products in the controller. To minimize reactor pressure drop and avoid internal heat and mass transport limitations, catalyst particles of 0.00013 to 0.00025 m diameter (60/100 mesh) were used.

On-line product analysis was performed by gas chromatography after 15 min on stream and then at one hour intervals. Samples were collected at elevated temperature and atmospheric pressure by using two gas

sampling valves with 0.0005-liter sample loops. All postreactor lines and valves were heated to reaction temperature in order to avoid product condensation. Organic products were separated with 0.00025-m-i.d., 30-m Supelco SPB-1 capillary column (split ratio = 80) and quantified using a flame ionization detector. Ar, CO, and CO_2 were separated on a Supelco S-2 carbosieve column and detected by thermal conductivity. H_2 and H_2O concentrations were not determined. Compound sensitivity factors for each detector were established experimentally and were in good agreement with those reported by Dietz (9). Both columns were located in a single oven, which was ramped from 263 to 553 K at 10 K/min for maximum product separation. Data were acquired and analyzed with a Spectra-Physics 4000 lab station.

For safe operation the reactor was designed to shut down automatically if hazardous levels of hydrogen or carbon monoxide were detected or if reactor overtemperature occurred. System over-pressure was protected against by placing a rupture disk assembly at the inlet of the reactor.

All reaction studies employed a H_2/CO/Ar synthesis gas of molar composition 2/1/0.5 at a gas hourly space velocity (STP) of 4000 hr^{-1}. Argon served as an internal standard for calculation of activity. Temperature and total pressure were maintained at 548 K and 5 MPa, respectively. Before synthesis gas exposure, the calcined catalysts were reduced *in situ* with a mixture of 10% H_2 in argon mixture at atmospheric pressure and 548 K. With this pretreatment procedure unpromoted cupric oxide was found by thermal gravimetric analysis to reduce completely to copper metal within 15 min. A small temperature gradient (5–10 K) passed quickly through the reactor during pretreatment. No temperature gradient was noted during synthesis gas reaction. Carbon monoxide conversions never exceeded 5 mol%, minimizing heat and mass transfer limitations. The equilibrium conversion of carbon monoxide to methanol was calculated to be 37 mol% at 548 K and 5 MPa.

Surface areas of the unsupported catalysts were calculated from multipoint BET adsorption isotherms of Kr at 77 K. A Micromeretics 2100E Accusorb surface area analyzer was used to obtain adsorption isotherms.

Powder X-ray diffraction patterns were obtained with an automated Picker theta–theta diffractometer using Mo$K\alpha$ radiation. The step size was 0.04° per step with a 3-sec per step counting time. Low area quartz (α-SiO_2) was used as an internal standard and was mixed with all samples at a 5 wt% concentration. The *d*-spacing of the (101) reflection was referenced to 3.342 Å.

We collected scanning electron micrographs by using a Jeol Model JSM-U3 scanning electron microscope. Energy-dispersive X-ray spectra were obtained with a Tracor/Northern 2000 microanalyzer. Samples were mounted on graphite stubs. Approximately 300 Å of gold was sputtered onto the samples to ensure adequate conductivity.

X-ray photoelectron spectra were obtained with an AEI 200B spectrometer using Al$K\alpha$ radiation ($h\nu$ = 1486.6 eV). Binding energies were assigned by referencing to the carbon 1*s* peak of adventitious carbon at 285.0 eV. Samples were prepared by loading the catalyst into soda-lime glass tubing, performing the appropriate treatment, and then evacuating and sealing the tubes. Both hydrogen and synthesis gas treatments were performed at atmospheric pressure. The tubes were transported to and opened in a helium dry box attached directly to the spectrometer. Samples were mounted by pressing the catalyst powder onto indium foil.

RESULTS

Reactor Studies

The surface areas after synthesis gas reaction of the various catalyst compositions tested are given in Table 1. The values are

TABLE 1

Composition and Surface areas of Cu–K Catalysts Prepared via Homogeneous Citrate Complexes

Molar composition	Mole fraction potassium[a]	Used catalyst surface area (m^2/g)
CuK_0	0	1.22
$CuK_{0.012}$	0.012	0.71
$CuK_{0.025}$	0.024	0.76
$CuK_{0.09}$	0.083	0.89
$CuK_{0.36}$	0.265	0.33

[a] Defined by mol K/(mol K + mol Cu).

similar to that reported for an unsupported copper catalyst prepared via a copper hydroxy nitrate precursor (*3*). A decrease in surface area is observed with increasing amounts of potassium promotion. A similar effect has been reported for alkali promotion of copper–zinc oxide catalysts (*5, 10*).

Catalytic activity and selectivity for carbon monoxide hydrogenation as a function of potassium content are plotted in Fig. 2. The results reported are the values found after the catalyst had been on stream for 10 hr. Methanol was produced immediately upon synthesis gas exposure, and the rates when normalized with respect to surface area varied little over the first 10 hr. Activities were normalized with respect to the surface area of used catalysts. The selectivity to methanol was high (93 to 98 wt%) with methane and carbon dioxide as the only by-products. As a comparison, cesium promoted copper–zinc oxide synthesis catalysts have selectivities of 99 wt% (*7*).

Umpromoted copper was found to be inactive for synthesis gas conversion. The incorporation of only 1.2 mol% of potassium with copper resulted in a catalyst that selectively (93 wt%) synthesized methanol at a rate of 8.3×10^{-5} kg/m^2/hr. Interestingly, increasing the mole fraction of potassium to 0.26, a 20-fold increase, resulted in an increase in catalytic activity by a factor of only 1.6.

In an effort to avoid the rapid decomposition associated with cupric nitrate catalyst precursors, we studied an alternative preparation method substituting cupric acetate for cupric nitrate. Also, to evaluate whether the citric acid complexation preparation method was necessary to impart the promotional effect of potassium on copper, we examined a potassium carbonate impregnated cupric oxide catalyst. In Table 2 the activities of these alternatively prepared catalyst are compared to a catalyst of similar composition prepared from cupric nitrate.

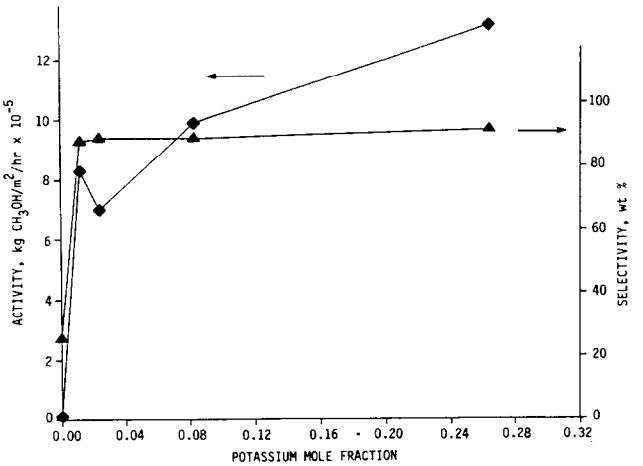

FIG. 2. Methanol activity and selectivity of potassium promoted copper catalysts.

TABLE 2

Activity of Alternate Preparations

Molar composition	Used catalyst surface area (m^2/g)	Methanol activity $kg/m^2hr \times 10^5$
$CuK_{0.025}$[a]	0.76	7.0
$CuK_{0.032}$[b]	0.63	1.7
$CuK_{0.032}$[c]	2.87	4.8

[a] Cupric nitrate preparation of homogeneous citrate complex.

[b] Cupric acetate preparation of homogeneous citrate complex.

[c] Potassium carbonate impregnation of cupric oxide.

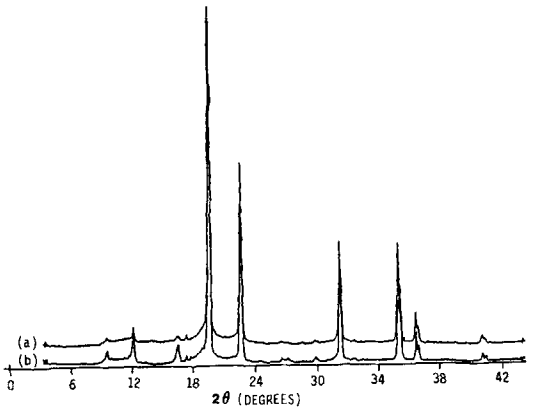

FIG. 3. Powder X-ray diffraction patterns: (a) reduced $CuK_{0.36}$ catalysts; (b) copper metal powder.

The catalyst prepared from cupric acetate was found to be less active by a factor of 4 than the catalyst prepared from cupric nitrate. It was noted during preparation of this catalyst that the complete dissolution of cupric acetate was not occurring. The potassium carbonate impregnated cupric oxide catalyst, on the other hand, had activity comparable to that of the cupric nitrate derived catalyst. The cupric oxide used for this preparation was found to be inactive for carbon monoxide hydrogenation. Hence, the promoting effect of potassium may be imparted through simple impregnation as well as the more involved citrate complex preparation previously outlined.

X-Ray Diffraction

The powder X-ray diffraction pattern for the used $CuK_{0.36}$ catalyst is shown in Fig. 3. For comparison, the pattern obtained for copper metal powder mixed with 5 wt% α-SiO_2 is also shown. Despite the large concentration of potassium, copper metal was the only observed phase. The *d*-spacings for the copper metal phase in the catalyst were in excellent agreement with those reported in the literature (*11*). Since no potassium phases were observed in any of the calcined, reduced, or used catalysts, the potassium is concluded to be in a microcrystalline (<20 Å) or amorphous phase.

X-Ray Photoelectron Spectroscopy

X-ray photoelectron spectra of the calcined, reduced, and synthesis-gas-exposed $CuK_{0.36}$ catalyst were collected. The binding energies of the Cu $2p_{3/2}$ photoemitted electrons are given in Table 3. The 933.0-eV binding energy for the calcined catalyst was assigned to Cu^{2+} species (*12*). The Cu $2p_{3/2}$ photoelectron spectrum of the calcined catalyst was observed to have a satellite peak at 941.2 eV. The appearance of a satellite peak is indicative of Cu^{2+} species (*13*). The reduced and synthesis-gas-exposed catalysts were found to have Cu $2p_{3/2}$ binding energies of 931.5 and 931.7 eV, respectively. These peaks were assigned to either Cu^+ or Cu^0 species (*12*). Differentiation of Cu^+ and Cu^0 species in XPS is possible only through examination of the $L_3M_{4,5}M_{4,5}$ X-ray-induced Auger transitions. Specifically, the difference in kinetic

TABLE 3

Cu $2p_{3/2}$ Binding Energies of $CuK_{0.36}$ Catalyst

Treatment	Binding energy (eV)
Calcined	933.0
Hydrogen reduced	931.5
Synthesis-gas-exposed	931.7

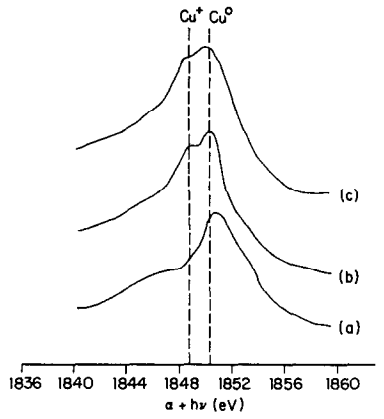

FIG. 4. $L_3M_{4,5}M_{4,5}$ X-ray-induced Auger transitions for $CuK_{0.36}$ catalyst: (a) calcined; (b) hydrogen reduced; (c) synthesis gas exposed.

energy of the X-ray-induced Auger transition and the $3p_{3/2}$ photoemitted electron is evaluated. This difference is referred to as the Auger parameter, α. Because the kinetic energy of the photoemitted electron is dependent upon the energy of the excitation source, $h\nu$, a modified Auger parameter defined by

$$\alpha + h\nu = KE_{LMM} - KE_{2p_{3/2}} + h\nu$$

is generally used. KE_{LMM} and $KE_{2p_{3/2}}$ are the kinetic energies of the $L_3M_{4,5}M_{4,5}$ X-ray-induced Auger emitted electrons and the $2p_{3/2}$ photoemitted electrons, respectively. The modified Auger parameter is independent of the excitation energy since $h\nu$-$KE_{2p_{3/2}}$ is simply the binding energy of the $2p_{3/2}$ photoemitted electron. The advantage of the Auger parameter is that static charge effects subtract out. The X-ray-induced Auger transitions for the calcined, reduced, and synthesis-gas-exposed $CuK_{0.36}$ catalyst are shown in Fig. 4. The calcined catalyst was found to have one peak at 1850.8 eV, while the reduced and synthesis-gas-exposed catalysts had two peaks at 1848.8 and 1850.6 eV, respectively. For comparison, the modified Auger parameters of copper(II) oxide, copper(I) oxide, and copper metal are reported to be 1850.9, 1848.9 and 1851.2 eV (*14*). Cu^{2+} and Cu^0 are indistinguishable by the Auger parameter. The position of the Auger transition for the calcined catalyst is in agreement with the Cu $2p_{3/2}$ spectrum that indicates only Cu^{2+} species. The reduced and synthesis-gas-exposed samples, which the Cu $2p_{3/2}$ spectra indicated to consist of either Cu^0 or Cu^+ species, had Auger transitions corresponding to both species. Hence, upon hydrogen exposure only part of the Cu^{2+} species in the calcined catalyst reduced to copper metal, with the remainder being stabilized in the Cu^+ state. Synthesis gas exposure did not significantly alter the Auger transitions of the reduced catalyst.

The carbon and potassium X-ray photoelectron spectrum for the reduced $CuK_{0.36}$ catalyst is shown in Fig. 5. The peaks at 292.9 and 296.0 eV were assigned to potassium $2p_{3/2}$ and $2p_{1/2}$ photoemitted electrons, respectively. Unfortunately, potassium compounds exhibit very little chemical shift so that information on the chemical state of potassium could not be obtained. The peak at 285.0 eV is the C 1*s* reference peak resulting from adventitious carbon. The small peak appearing at 289.2 eV has been assigned to C 1*s* in a carbonate structure. For comparison, the X-ray photoelectron spectrum of potassium carbonate is also plotted in Fig. 5. The similarity of the potassium and carbonate peak intensities suggests that

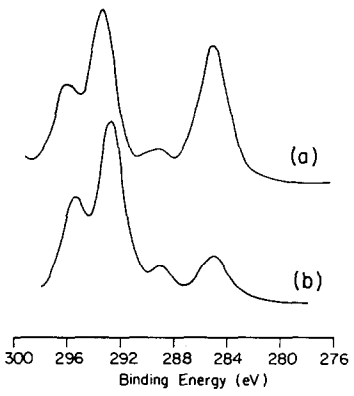

FIG. 5. Carbon and potassium X-ray photoelectron spectra: (a) $CuK_{0.36}$ catalyst; (b) potassium carbonate.

most of the potassium in the catalyst is in the carbonate form. This possibility will be discussed in detail later.

Comparison of Alternate Preparations

This disparity in the methanol synthesis rates of the cupric nitrate and cupric acetate prepared catalysts prompted us to investigate these preparations in further detail. X-ray photoelectron spectroscopy in the Cu $2p_{3/2}$ region revealed only one peak at a binding energy of 931.8 eV for the reduced catalysts. As before, this was assigned to Cu^+ or Cu^0 species. The Cu $L_3M_{4,5}M_{4,5}$ X-ray-induced Auger transitions for the reduced catalysts are compared in Fig. 6. The concentration of Cu^+ species relative to Cu^0 was observed qualitatively to be considerably less for the cupric acetate prepared catalyst. Scanning electron microscopy and energy-dispersive spectroscopy of the two preparations revealed distinct differences as shown in Figs. 7 and 8. Copper particles in the catalyst prepared with cupric nitrate appear to have small crystallites (75–150 nm) or "warts" dispersed over them. The morphology and energy-dispersive spectrum for the copper particle shown in Fig. 7 was found to be representative of the entire sample. Although the resolution of energy-dispersive spectroscopy does not permit chemical identification of these small crystallites, experiments on alkali promoted silver catalysts have revealed a similar morphology. Auger spectroscopy showed that the "warts" on the promoted silver catalysts were composed of alkali (*15*). The catalyst prepared from cupric acetate is much different in that it contains patches of a needle structure. Other areas on this catalyst were similar in morphology to the cupric nitrate prepared catalyst. The energy-dispersive spectra of the areas with and without the needle clusters indicate that the clusters are enriched in potassium, while "needle free" areas have less potassium than that for the cupric nitrate prepared catalyst.

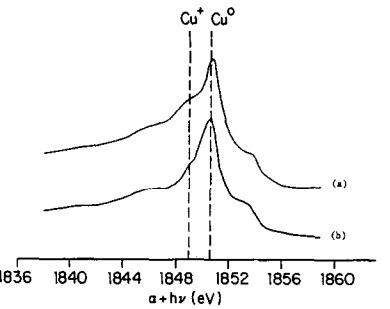

FIG. 6. $L_3M_{4,5}M_{4,5}$ X-ray-induced Auger transitions for citrate complex prepared catalysts in reduced state: (a) cupric nitrate precursor; (b) cupric acetate precursor.

DISCUSSION

As expected, the unpromoted copper catalyst was inactive for carbon monoxide hydrogenation, and no promotion attributable to the preparation technique itself was observed. We evaluated the catalytic behavior of reagent grade potassium carbonate as well and found that it too is inactive. Hence, there is truly a synergistic effect involved in the synthesis of methanol on unsupported potassium–copper catalysts.

Nunan and co-workers (*7*) have reported a methanol synthesis rate of 0.56 kg/kg cat./hr at 523 K and 7.6 MPa with a synthesis gas ratio of 2.333 when a copper–zinc oxide catalyst impregnated with 0.8 mol% Cs is used. The methanol synthesis rate was observed to pass through a maximum at the 0.8 mol% promotion amount. If we use an activation energy correction of 18.3 kcal/mol (*7*) a linear total pressure correction (*16*), and a surface area of 18.8 m^2/g (*5*), the methanol synthesis rate is 4.4×10^{-5} $kg/m^2/hr$ under the conditions used in our study. This is a factor of 2 lower than the 8.3×10^{-5} $kg/m^2/hr$ methanol synthesis rate found here for a 1.2 mol% potassium promoted, unsupported copper catalyst. In addition, we have found no decrease in catalytic activity even with 26 mol% potassium in the catalyst. It is probable that the preparation method used here increases the dispersion of potassium throughout the catalyst and as

(a)

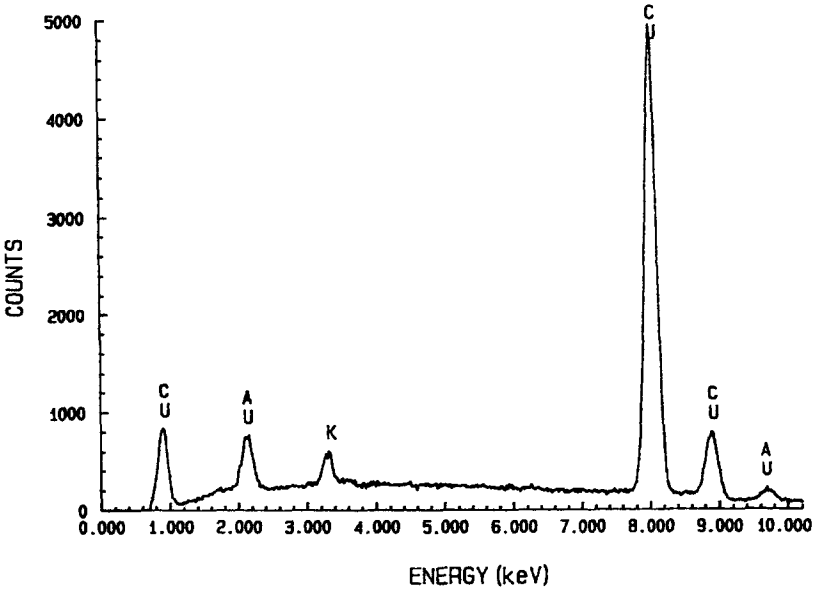

(b)

FIG. 7. Scanning electron microscopy and energy-dispersive spectroscopy of reduced cupric nitrate prepared catalyst: (a) scanning electron micrograph; (b) energy-dispersive spectrum.

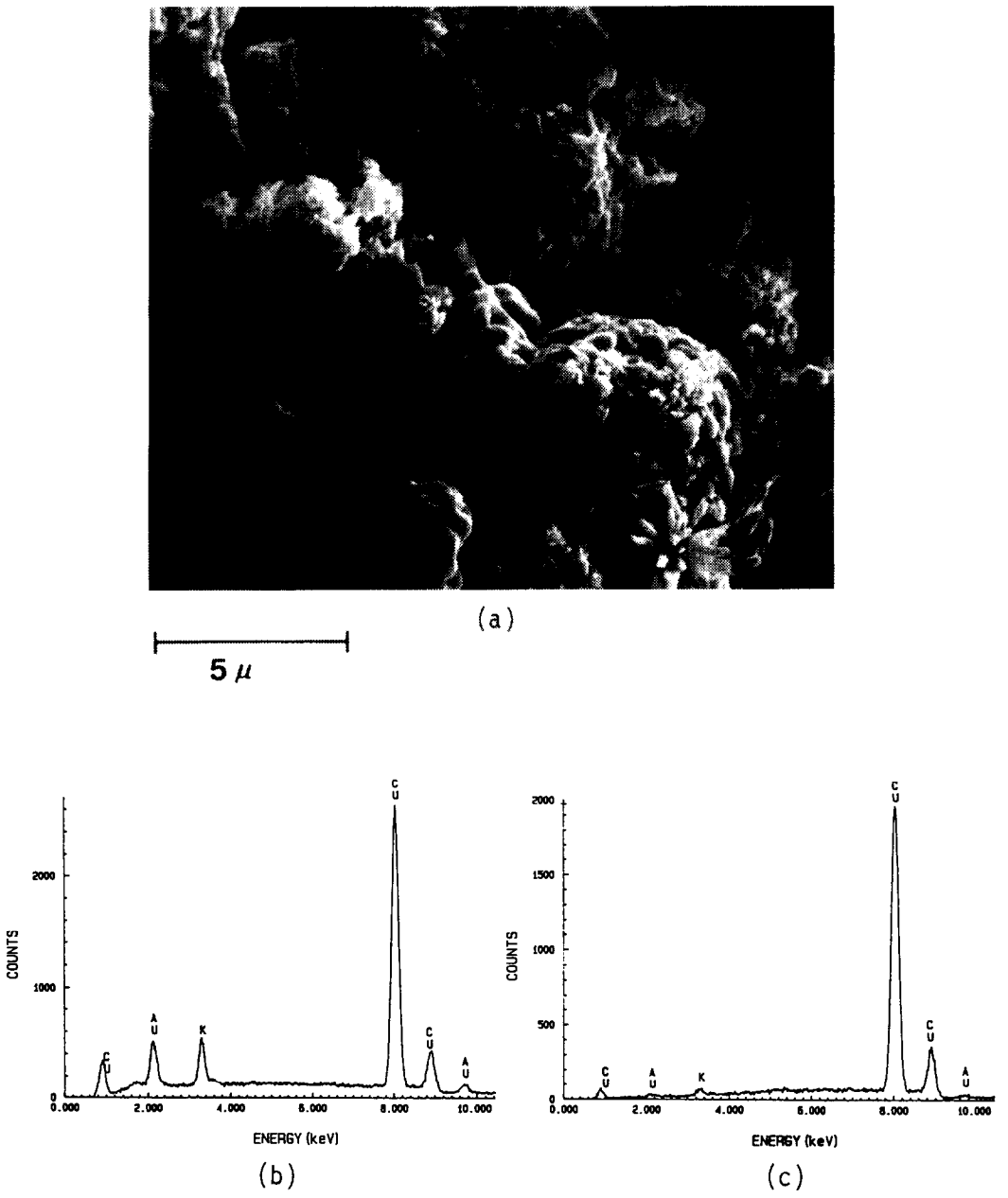

FIG. 8. Scanning electron microscopy and energy-dispersive spectroscopy of reduced cupric-acetate-prepared catalyst: (a) scanning electron micrograph; (b) energy-dispersive spectrum collected in area of needle clusters; (c) energy-dispersive spectrum collected in area away from needle clusters.

a result suppresses active site blocking that can occur with impregnation methods where the promoter is distributed only on the surface.

X-ray photoelectron spectroscopy results indicated that the calcined catalyst contains only Cu^{2+} species, which upon hydrogen exposure are reduced to a mixture of Cu^{+} and Cu^{0} species. Since unsupported copper metal was inactive for carbon mon-

oxide hydrogenation, the Cu^+ species must be responsible for the initiation of catalytic activity observed with the potassium promoted unsupported copper catalysts. Methanol synthesis activity has been correlated with the existence of cuprous ions in copper–chromium oxide catalysts (*17*) and in copper–zinc oxide catalysts (*14, 18*) as well. In both cases, the second component stabilizes Cu^+ species by phase formation. In Cu–Cr oxide, this is achieved by formation of $CuCrO_2$ (*19*), while in copper–zinc oxide, the Cu^+ species occupy substitutional and/or interstitial sites in the zinc oxide lattice (*18*). The mechanism by which potassium stabilizes cuprous ions on unsupported copper catalysts could not be elucidated with the characterization techniques used in this study. In particular, no cuprous or potassium phases were detected in the powder X-ray diffraction pattern even with 26 mol% potassium in the catalyst. If phase formation (between copper and potassium) was responsible for Cu^+ stabilization, then a literature review suggests one possibility, KCuO, which has been synthesized by Hestermann and Hoppe (*20*).

Another possibility, $KCuCO_3$, is suggested by analogy to the results of a study of cesium-promoted copper catalysts by NMR of ^{133}Cs (*21*). Cesium was found to stabilize Cu^+ by substitution into an alkali carbonate structure in the same way as several other mixed carbonate salts: $NaAgCO_3$, $KAgCO_3$, and $RbAgCO_3$ (*22*). The presence of phase formation would help to explain why the activity varies little when the concentration of potassium in the catalyst is changed by a factor of 20. With surface areas of the order of 1 m^2/g, a potassium concentration of as little as 0.012 mole fraction could result in as many as six monolayers of potassium if atomically dispersed.

The importance of obtaining thorough mixing and maximum contact of potassium and copper is clearly demonstrated by the alternative preparation that uses cupric acetate in place of cubric nitrate. As the SEM/EDS and XPS data indicate, the concentration of potassium into needle clusters on the surface resulted in a decrease in the amount of Cu^+ species at the surface and a subsequent decrease in catalytic activity. The poorer potassium dispersion in this catalyst probably resulted from the poor water solubility of cupric acetate, as noted earlier. The ability to promote methanol synthesis on cupric oxide by potassium carbonate impregnation demonstrates that this preparation method may be used to obtain the necessary potassium–copper interaction and may suggest that copper on a high surface area support would also be promoted by potassium impregnation.

As an alternative to the current work, which normalizes activity with respect to surface area, future works should attempt to examine activity with respect to the number of surface Cu^+ sites determined, perhaps, by CO adsorption along with TPD or FTIR. Normalized with respect to the number of surface Cu^+ sites, the activity of each of the three preparation methods may be equal.

The chemical state of potassium in the unsupported copper catalysts was suggested by XPS to be potassium carbonate. Experimentally we found that potassium citrate, the probable potassium phase precursor when citric acid complexation preparation methods are used, decomposed to potassium carbonate when calcined. As noted in the Introduction, it has been proposed for alkali promoted copper–zinc oxide catalysts that the rate of methanol synthesis is increased as a result of carbon monoxide reaction with alkali hydroxide to produce alkali formate species that are hydrogenated to methanol. Since the characterization techniques used in our study could neither confirm nor discount the presence of potassium hydroxide, thermodynamic calculations were performed to provide further insight into the chemical nature of potassium under synthesis gas conditions. The reactions of interest are

$$2KOH + CO \rightarrow K_2CO_3 + H_2, \quad \Delta G^0_{573\,K} = -35 \text{ kcal/mol}$$

$$K_2O_2 + CO \rightarrow K_2CO_3, \quad \Delta G^0_{573\,K} = -109 \text{ kcal/mol}$$

$$K_2O + 2CO + 2H_2 \rightarrow K_2CO_3 + CH_4, \quad \Delta G^0_{573\,K} = -96 \text{ kcal/mol}.$$

Since the reaction of all other potassium compounds with synthesis gas to form potassium carbonate results in a decrease in free energy, potassium carbonate is the thermodynamically stable phase under synthesis gas at reactor temperature. To confirm the above results, we exposed potassium hydroxide to synthesis gas for 12 hr at 573 K. The product was identified as potassium carbonate by X-ray diffraction and wet chemistry.

Since bulk potassium hydroxide is not stable under synthesis gas conditions, its role at the surface in enhancing the methanol synthesis rate by promoting the formation of formate species is questioned. The results of our work suggest that potassium interacts with copper to increase the concentration of Cu^+ active sites.

SUMMARY

It has been found that potassium does promote unsupported copper catalysts for the selective synthesis (>93 wt%) of methanol from synthesis gas. The methanol synthesis rate, 8.3×10^{-5} kg/m^2/hr, was twice that calculated by extrapolation of the results for cesium promoted copper–zinc oxide catalysts.

The chemical state of both copper and potassium was investigated. X-ray photoelectron spectroscopy results indicated that the calcined catalysts contain only Cu^{2+} species, which upon hydrogen exposure are reduced to a mixture of Cu^+ and Cu^0 species. Since copper metal alone was inactive for carbon monoxide hydrogenation, the initiation of methanol synthesis activity on the promoted catalysts correlated with the stabilization of the Cu^+ species. The chemical state of potassium appeared to be potassium carbonate, which was shown to be the thermodynamically preferred phase under reaction conditions.

Since alkali hydroxides are unstable under reaction conditions, the synthesis of methanol by the hydrogenation of alkali formate intermediates formed through the reaction of carbon monoxide with alkali hydroxide is discounted as the source of the promotional effect. Instead, the promotional effect of potassium on copper is the result of the ability of potassium to stabilize Cu^+ species, perhaps through phase formation upon catalyst reduction.

ACKNOWLEDGMENTS

We gratefully acknowledge the receipt of start-up funds from the Shell Companies Foundation, Faculty Initiation Fund. One of the authors (G.R.S.) thanks the Amoco Foundation for fellowship support. In addition we thank Dr. Robert Jacobson (Ames Laboratory) for use of the X-ray diffractometer and James Anderegg (Ames Laboratory) for assistance in X-ray photoelectron spectra collection.

REFERENCES

1. Audibert, E., and Raineau, A., *Ind. Eng. Chem.* **11,** 1105 (1928).
2. Eguchi, T., *Fuel Economist* **11,** 417 (1936).
3. Klier, K., "Advances in Catalysis," Vol. 31, p. 243. Academic Press, New York, 1982.
4. Vedage, G. A., Himelfarb, P. B., Simmons, G. W., and Klier, K., *in* "Solid State Chemistry in Catalysis," ACS Symposium Series 279, pp. 295–312. American Chemical Society, Washington, DC, 1985.
5. Klier, K., *Appl. Surf. Sci.* **19,** 267 (1984).
6. Klier, K., *in* "Catalysis on the Energy Scene" (S. Kaliaguine and A. Mahay, Eds.), pp. 439–455. Elsevier, Amsterdam, 1984.
7. Nunan, J. C., Klier, K., Young, C.-W., Himelfarb, P. B., and Herman, R. G., *J. Chem. Soc. Chem. Soc. Chem. Commun.,* 193 (1986).
8. Courty, P., Durand, D., Freund, E., and Sugier, A., *J. Mol. Catal.* **17,** 241 (1982).
9. Dietz, W. A., *J. Gas Chromatogr.* 5(2), 68 (1967).
10. Smith, K. J., and Anderson, R. B., *Canad. J. Chem. Eng.* **61,** 40 (1983).
11. Joint Committee on Powder Diffraction Standards, file number 4-836.
12. "Handbook of X-Ray Photoelectron Spectroscopy" (G. C. Muilenberg, Ed.). Physical Electronics, Eden Prairie, MN, 1976.

13. Frost, D. C., McDowell, C. A., and Ishitani, A., *Mol. Phys.* **24,** 861 (1972).
14. Karwaci, E. J., Anewalt, M. R., and Brown, D. M., *Prepr. Div. Fuel Chem. Amer. Chem. Soc.* **29,** 210 (1984).
15. Mross, W. D., *Catal. Rev. Sci. Eng.* **25,** 591 (1983).
16. Agny, R. M., and Takoudis, C. G., *Ind. Eng. Chem. Prod. Res. Dev.* **24,** 50 (1985).
17. Monnier, J. R., Hanrahan, M. J., and Apai, G. R., *J. Catal.* **92,** 119 (1985).
18. Herman, R. G., Klier, K., Simmons, G. W., Finn, B. P., Bulko, J. B., and Kobylinski, T. P., *J. Catal.* **56,** 407 (1979).
19. Apai, G. R., Monnier, J. R., and Hanrahan, M. J., *J. Chem. Soc. Chem. Commun.,* 212 (1984).
20. Hestermann, K., and Hoppe, R., *Z. Anorg. Allg. Chem.* **360,** 113 (1968).
21. Chu, P. J., Gerstein, B. C., Sheffer, G. R., and King, T. S., *J. Catal.,* in press.
22. Papin, G., Christmann, M., and Sadeghi, N., *C. R. Acad. Sci. Paris* **284,** 791 (1977).